Fixed-Complexity Quantum-Assisted Multi-User Detection for CDMA and SDMA

Panagiotis Botsinis, *Student Member, IEEE,* Soon Xin Ng, *Senior Member, IEEE,* and Lajos Hanzo, *Fellow Member, IEEE*

***Abstract*—In a system supporting numerous users the complexity of the optimal Maximum Likelihood Multi-User Detector (ML MUD) becomes excessive. Based on the superimposed constellations of K users, the ML MUD outputs the specific multi-level K-user symbol that minimizes the Euclidean distance with respect to the faded and noise-contaminated received multi-level symbol. Explicitly, the Euclidean distance is considered as the Cost Function (CF). In a system supporting K users employing M-ary modulation, the ML MUD uses M^K CF evaluations (CFE) per time slot. In this contribution we propose an Early Stopping-aided Dürr-Høyer algorithm-based Quantum-assisted MUD (ES-DHA QMUD) based on two techniques for achieving optimal ML detection at a low complexity. Our solution is also capable of flexibly adjusting the QMUD's performance and complexity trade-off, depending on the computing power available at the base station. We conclude by proposing a general design methodology for the ES-DHA QMUD in the context of both CDMA and SDMA systems.**

***Index Terms*—Code division multiple access, computational complexity, Dürr-Høyer Algorithm, Grover's Quantum Search Algorithm, multiuser detection, quantum computing, spatial division multiple access.**

I. Introduction

In the uplink of a wireless Code Division Multiple Access (CDMA) communication system that supports multiple users, Multi-User Detection (MUD) [1] is essential. The optimal Maximum Likelihood (ML) MUD [1] of a system supporting K users and employing M-ary modulation requires M^K evaluations of a Cost Function (CF). When M and K are large, the vast number of CF evaluations (CFE) may become excessive. Apart from CDMA systems, the minimization of a CF is necessary for example in Spatial Division Multiple Access (SDMA) Multiple-Input Multiple-Output (MIMO) systems [2], in MIMO-aided Orthogonal Frequency-Division Multiplexing (OFDM) systems [3], [4] and in cooperative multi-cell systems, where the Base Stations (BS) of multiple cells are connected by optical fibre [5]. Furthermore, low-complexity optimization algorithms are also needed both in power-control and in resource allocation [6]–[8], as well as in finding the optimal routes in large-scale multi-hop networks [9]–[12]. As an application scenario, our proposed quantum-assisted detection methodology will be investigated in the context of the uplink of MUD-aided Direct-Sequence (DS) CDMA and SDMA systems relying on multiple receive antennas.

Quantum computation exploits the postulates of quantum mechanics [13]–[15], enabling the realization of potentially non-intuitive processes that cannot be implemented in classic computers, as exemplified by quantum parallelism [13] and quantum entanglement [13]. An example of efficient quantum-processing is constituted by Grover's Quantum Search Algorithm (QSA) [16], which performs a search in an unsorted database having N elements by requiring as few as $O(\sqrt{N})$ database queries. By contrast, the classic full-search algorithm needs $O(N)$ database queries [16]. Based on a given value δ, a search algorithm finds an x so that $f(x) = \delta$. The index x that satisfies $f(x) = \delta$ is termed as the *solution*. However, Grover's QSA succeeds only if a single solution exists in the database/function. Hence Boyer, Brassard, Høyer and Tapp (BBHT) proposed the BBHT QSA in [17] as a generalization of Grover's QSA that finds a solution using as few as $O(\sqrt{N})$ CFEs, even if multiple solutions exist and even if the *a priori* knowledge of the exact number of solutions is unavailable. As a further advance, Dürr and Høyer conceived a quantum algorithm termed as the Dürr-Høyer Algorithm (DHA) for finding the index of the specific solution in the search-space that minimizes a CF having N different legitimate inputs using $O(\sqrt{N})$ CFEs at an almost 100% probability of success [18]. A Quantum Genetic Optimization Algorithm (QGOA) was proposed in [19], where the offsprings of each generation were chosen according to the output of a few iterations of the DHA invoked for creating more fit offsprings.

In lightly-loaded ($K < SF$) and full-rank ($K = SF$) CDMA systems relying on a spreading factor of SF, the conventional Matched Filter (MF) detector has an adequate performance. By contrast, in rank-deficient ($K > SF$) systems, the MF detector fails to reliably estimate the transmitted M^K-level symbol. In fact, as the ratio K/SF becomes higher, the MF output becomes equivalent to a random guess [1]. Other reduced-complexity MUDs, such as the Minimum Mean-Square Error (MMSE) MUD [20] and the Minimum BER (MBER) MUD [21], experience a similar behaviour. The Zero-Forcing (ZF) detector and the MMSE detector of SDMA systems also perform sub-optimally, albeit their performance approaches that of the ML MUD, when the number of users

Manuscript received August 6, 2013; revised November 20, 2013. The editor coordinating the review of this paper and approving it for publication was S. Affes.

The authors are with the School of Electronics and Computer Science, University of Southampton, Southampton, SO17 1BJ, UK (e-mail: {pb8g10, sxn, lh}@ecs.soton.ac.uk).

The financial support of the RC-UK under the India-UK Advanced Technology Centre (IU-ATC), of the EU under the Concerto project and that of the European Research Council, Advanced Fellow Grant and of the Royal Society's Wolfson Reasearch Merit Award is gratefully acknowledged.

Digital Object Identifier 10.1109/TCOMM.2014.012514.130615

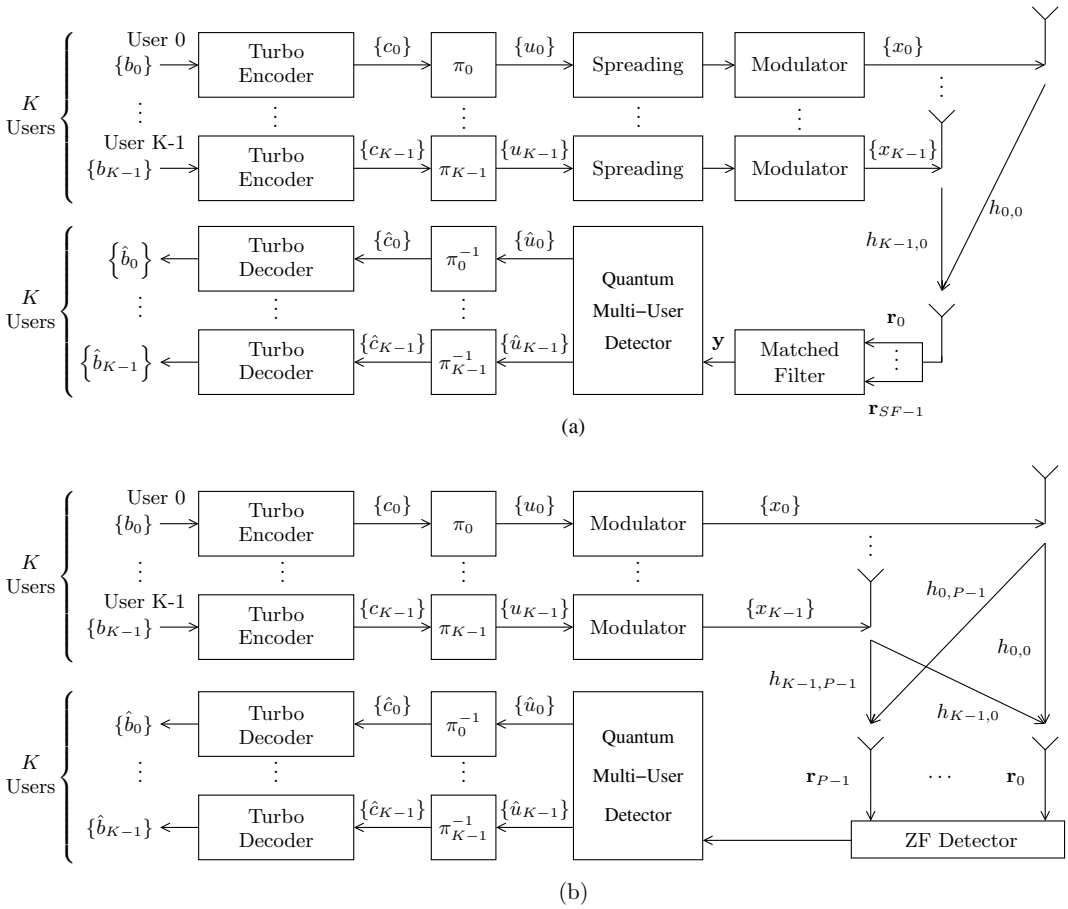

Fig. 1. (a) DS-CDMA and (b) SDMA uplink communication system's block diagram supporting K users employing turbo encoding using two convolutional codes as well as non-iterative, hard-output QMUD at the BS.

K becomes lower than the number of receive antennas P. Apart from the heuristic algorithms of [22]–[25], which are capable of achieving a near-optimal MUD performance [1], quantum-assisted MUDs (QMUD) may also be used in classic CDMA and SDMA systems for optimal detection at a low complexity, especially in rank-deficient systems, where we have $K/SF > 1$ and $K/P > 1$, respectively. The inputs and outputs of a Quantum-assisted MUD belong to the Classic Domain (CD), while their internal processes take place in the Quantum Domain (QD). Imre and Balázs [26] conceived a hard-input hard-output QMUD associated with a complexity of $O(\sqrt{N})$ database queries, where N is the search space's size. In our prior research we proposed a soft-input soft-output (SISO) QMUD [27] having a complexity of $O(\sqrt{N})$, which is achieved by combining the DHA [18] and the Quantum Weighted Sum Algorithm (QWSA) proposed in [27]. Furthermore, the DHA was also employed in [27] for creating a non-iterative, hard-decision QMUD, which achieved a performance identical to that of the classic ML MUD at a complexity of $O(\sqrt{N})$ CFEs. Hence this solution may be viewed as the QD-equivalent of the ML MUD. The exact computational complexity of the QMUD proposed in [27] during each detection iteration may vary, making it unattractive in applications, where having a fixed complexity is essential.

Against this background, our novel contributions are:

1) *We propose a fixed-complexity hard-input hard-output QMUD based on the novel Early-Stopping aided (ES) DHA, achieving an optimal performance at a fixed computational complexity, which is lower than that of the DHA QMUD proposed in [27].*
2) *We conceive a flexible ES-DHA based QMUD design methodology capable of meeting a specific BER performance target within a certain complexity-constraint. Our QMUD is capable of supporting severely rank-deficient DS-CDMA and SDMA systems.*
3) *We demonstrate the impact of the initial MF output of the DS-CDMA arrangement and that of the ZF as well as MMSE detectors of the SDMA systems on the proposed DHA.*

The rest of the paper is structured as follows. The communication systems considered are presented in Section II, while Section III introduces Grover's QSA, the BBHT QSA and the deterministically-initialized, ES-aided DHA. Our design methodology is presented in Section IV followed by the complexity and performance results in Section V. Finally, our conclusions are offered in Section VI.

II. System Overview

A. DS-CDMA system

The CDMA uplink considered supports K users, as seen in Fig. 1a. The kth user's, $k = 0, \ldots, K-1$, information

bit stream $\{b_k\}$ is encoded into the bit stream $\{c_k\}$, which is interleaved by the bit-based interleavers. The user-specific DS-CDMA spreading sequences are used for spreading the interleaved bit sequences $\{u_k\}$, before modulating them onto M-ary symbols using Gray mapping. Furthermore, the modulated symbol stream $\{x_k\}$ is transmitted over an uncorrelated Rayleigh fading channel over T time slots. We assume perfect estimation of the channel matrix $\mathbf{H}$ at the Base Station (BS). Moreover, the knowledge of the DS-CDMA codebook $\mathbf{C} = [\mathbf{c}_0, \ldots, \mathbf{c}_{K-1}]$ associated with $\mathbf{c}_k = [c_{k,0}, \ldots, c_{k,SF-1}]^T$ and the Spreading Factor (SF) is also assumed at the BS. Naturally, the thermal noise imposed at the BS's antenna is unknown.

The MF of the BS accepts as its inputs K number of received signals during a specific chip period, leading to the MF output

$$\begin{aligned}\mathbf{y} &= \mathbf{C}^H\mathbf{C}\mathbf{H}\mathbf{x} + \mathbf{C}^H\mathbf{n} \\ &= \mathbf{R}\mathbf{x} + \tilde{\mathbf{n}},\end{aligned} \tag{1}$$

where $\mathbf{y} = [y_0, \ldots, y_{K-1}]^T$ contains each user's MF output, $\mathbf{x} = [x_0, \ldots, x_{K-1}]^T$ is the transmitted M^K-ary multi-level symbol, $\mathbf{n} = [n_0, \ldots, n_{SF-1}]^T$ includes the noise samples experienced during each chip period, while $\mathbf{R} = \mathbf{C}^H\mathbf{C}\mathbf{H}$ and $\tilde{\mathbf{n}} = \mathbf{C}^H\mathbf{n} = [\tilde{n}_0, \ldots, \tilde{n}_{K-1}]^T$. In our DS-CDMA systems we will always assume a single receive antenna at the BS.

The Euclidean Distance (ED) between the received multi-level signal $\mathbf{y}$ and the legitimate, noise-free but faded, potentially received multi-level symbols $\mathbf{Rx}$, associated with the M^K-ary symbols $\mathbf{x}$, is used for formulating the probability of receiving $\mathbf{y}$, given that $\mathbf{x}$ was transmitted, which results in our CDMA CF of:

$$f_{CDMA}(\mathbf{x}) = \|\mathbf{y} - \mathbf{R}\mathbf{x}\|^2. \tag{2}$$

Both the classic ML MUD and the hard-output DHA-based QMUD of [27] find the specific symbol $\mathbf{x}_{\min}$ that minimizes the CF in (2). The MUD-process is symbol-based. The kth demodulated bit stream $\{\hat{u}_k\}$ is bit-deinterleaved and the resultant bit stream $\{\hat{c}_k\}$ is fed to the decoder. Finally, the output $\{\hat{b}_k\}$ of the turbo decoder is the estimate of the kth user's information bits.

B. SDMA system

The model of an SDMA system's uplink is presented in Figure 1b. Initially, the information bit stream $\{b_k\}$, $k \in \{0, 1, \ldots, K-1\}$, of each user is encoded into the bit stream $\{c_k\}$. After interleaving, the resultant bit stream $\{u_k\}$ of Fig. 1b is modulated onto the symbol stream $\{x_l\}$. The K users transmit their respective symbol stream simultaneously, each using a single antenna. The users are also assumed to be physically separated, therefore the non-dispersive Rayleigh channels spanning from the different transmit antennas are assumed to be uncorrelated. At the BS, the signal received during a single time slot may be described as

$$\mathbf{r} = \mathbf{H}\mathbf{x} + \mathbf{n}, \tag{3}$$

where $\mathbf{r} = [r_0, r_1, \ldots, r_{P-1}]^T$ includes the signal received at each of the receive antennas, $\mathbf{H} \in \mathbb{C}^{P \times K}$ is the channel matrix containing the CSI of each channel, $\mathbf{x} = [x_0, x_1, \ldots, x_{K-1}]^T$ is the transmitted multi-level symbol vector and $\mathbf{n} = [n_0, n_1, \ldots, n_{P-1}]^T$ contains the AWGN imposed at each of the P antennas at the BS. The channel matrix $\mathbf{H}$ is assumed to be perfectly estimated at the BS. The CF of the SDMA system is:

$$f_{SDMA}(\mathbf{x}) = \|\mathbf{r} - \mathbf{H}\mathbf{x}\|^2. \tag{4}$$

The QMUD of Figure 1b may receive as its input the signals of each receive antenna and an initial M^K-ary guess is formulated, which may even be random or may be provided by a low-complexity linear detector, such as the ZF or the MMSE detector. The estimation of the M^K-ary symbol is then performed by multiplying the received signal $\mathbf{r}$ by a complex-valued MUD weight matrix W as in

$$\hat{\mathbf{x}} = \mathbf{W}^H\mathbf{r}. \tag{5}$$

For the ZF detector we use the pseudo-inverse of the channel matrix[1] which is formulated as $\mathbf{W}^H = \mathbf{H}^+$, while the MMSE detector employs $\mathbf{W}^H = \left(\mathbf{H}^H\mathbf{H} + N_0\mathbf{I}\right)^{-1}\mathbf{H}^H$ for $K \leq P$ and $\mathbf{W}^H = \mathbf{H}^H\left(\mathbf{H}\mathbf{H}^H + N_0\mathbf{I}\right)^{-1}$ for $K > P$ [2].

III. Quantum Algorithms

In quantum computation the smallest unit of information is the quantum bit or *qubit* [13]. A qubit $|q\rangle$ may be found in any superposition of the states $|0\rangle$ and $|1\rangle$, as in $|q\rangle = a|0\rangle + b|1\rangle$, with $|a|^2 + |b|^2 = 1$, where $a, b \in \mathbb{C}$. In this paper[2] we will only consider real values for a and b. When a *measurement* takes place on the computational basis $\{|0\rangle, |1\rangle\}$, the observed qubit returns to either the $|0\rangle$ state with a probability of $|a|^2$ or the $|1\rangle$ state with probability $|b|^2$.

Two qubits may be found in the general quantum state $|q_1\rangle \otimes |q_2\rangle = (x|0\rangle + y|1\rangle) \otimes (w|0\rangle + z|1\rangle)$, where $\otimes$ is the tensor product, $|x|^2 + |y|^2 = 1$ and $|w|^2 + |z|^2 = 1$. The same quantum system may be described as $a|00\rangle + b|01\rangle + c|10\rangle + d|11\rangle$, where $|a|^2 + |b|^2 + |c|^2 + |d|^2 = 1$, $a = x \cdot w$, $b = x \cdot z$, $c = y \cdot w$ and $d = y \cdot z$. The value of $|a|^2 + |b|^2 = |x|^2$ represents the probability of the first qubit to be found in the $|0\rangle$ state after its observation. If the two qubits are superimposed in the quantum state $a|00\rangle + b|11\rangle$, then they are considered as *entangled*, since they cannot be described separately [13].

The state of a qubit evolves by applying a unitary operator U [13]. The Hadamard gate H [13] maps $|0\rangle$ to $|+\rangle = \frac{1}{\sqrt{2}}(|0\rangle + |1\rangle)$ and $|1\rangle$ to $|-\rangle = \frac{1}{\sqrt{2}}(|0\rangle - |1\rangle)$, creating in both cases an equiprobable superposition of the two states.

In our QMUD scenario, we have $N = M^K$ legitimate inputs to the CF. The potential solution index $x \in \{0, \ldots, M^K - 1\}$ is the decimal representation of the K users' M-bit symbols. For example, if we have $M = 4$ as well as $K = 2$ and Gray mapping is used, then $\mathbf{x} = [+1 + j, -1 + j]^T$ demodulates into $[00|10]$, hence $x = 2$.

A. Grover's Quantum Search Algorithm

Grover's QSA [16], [27] prepares an equiprobable superposition of all the possible multi-level symbols by passing

[1] In under-loaded and full-rank systems where $K \leq P$ we define $\mathbf{H}^+ = \left(\mathbf{H}^H\mathbf{H}\right)^{-1}\mathbf{H}^H$, while in rank-deficient systems we have $\mathbf{H}^+ = \mathbf{H}^H\left(\mathbf{H}\mathbf{H}^H\right)^{-1}$.

[2] For an extensive tutorial on quantum computing and the presented quantum algorithms please refer to [27].

$n = \log_2 M^K$ qubits assuming the $|0\rangle$ state through Hadamard gates [13], resulting in

$$|\gamma\rangle = \sum_{q=0}^{N-1} \frac{1}{\sqrt{N}}|q\rangle = \sum_{q=0}^{M^K-1} \frac{1}{\sqrt{M^K}}|q\rangle. \quad (6)$$

The number of solutions S in f has to be known *a priori* in order for Grover's QSA to succeed. Grover's QSA proposed in [16] was conceived for $S = 1$, but this constraint was relaxed to $S \geq 1$ in [17]. The Grover operator may be described as $\mathcal{G} = HP_0H \cdot O$, where H is the Hadamard gate [13], P_0 is a rotation gate [16] which maps $|x\rangle \rightarrow -|x\rangle$ if and only if $|x\rangle \neq |0\rangle$, and O is the so-called Oracle [16], [27]. The Oracle uses an auxiliary qubit in the $|-\rangle$ state and maps $|q\rangle$ to $-|q\rangle$ if $f(q) = \delta$ and keeps $|q\rangle$ unaltered, if $f(q) \neq \delta$. The Oracle marks the solutions by evaluating f in parallel. Since the computational complexity of the Oracle's operation will depend on the technology available, we will proceed by assuming that it is equivalent to 1 CFE [16], [17]. The Grover operator $\mathcal{G}$ is applied to $|\gamma\rangle$

$$L_{opt} = \lfloor \pi/4\sqrt{N/S} \rfloor \quad (7)$$

number of times [16]. When the resultant state $\mathcal{G}^{L_{opt}}|\gamma\rangle$ is observed in the $\{|0\rangle, |1\rangle\}^{\otimes n}$ basis, the probability of obtaining a solution is

$$P_{success} = \sin^2\left[(2L_{opt} + 1)\theta\right], \quad (8)$$

where we have [16]

$$\theta = \arcsin\sqrt{S/N}. \quad (9)$$

B. BBHT Quantum Search Algorithm

The BBHT QSA [17] does not require *a priori* knowledge of the number of solutions S in the database. It succeeds by applying $\mathcal{G}$ a pseudo-random number of times at the initial state $|\gamma\rangle$ in (6), observing the resultant state and repeating the application of $\mathcal{G}$ until a legitimate solution is obtained after the observation. If we have $S \neq 0$, the BBHT QSA associated with $\lambda = 6/5$ manages to find a solution after $L_{BBHT}^{QD,\ \max} = 4.5\sqrt{N/S}$ Grover iterations in the worst-case scenario [17], otherwise it is concluded that $S = 0$. The BBHT QSA is formally stated in Algorithm 1 [17], [27].

The variable L_{BBHT}^{QD} corresponds to the number of Grover iterations, or, equivalently, CFEs performed in the QD by the Oracle, where the CF was formulated in (2) and (4) for DS-CDMA and SDMA systems, respectively. By contrast, L_{BBHT}^{CD} keeps track of the number of CFEs performed in the CD in (2) and (4). At the current state-of-the-art in QD implementations it is impractical to compose the complexity of a CFE in the QD and CD. Hence we simply use the number of CF evaluations for quantifying the complexity. As and when necessary, we will take into account the total number of CFEs in both domains as $L_{BBHT} = L_{BBHT}^{CD} + L_{BBHT}^{QD}$ for the sake of providing comparisons with the family of classic MUDs. The number of CFEs in the CD during a single iteration of the BBHT QSA is equal to one, and it is performed in Step 5 of Algorithm 1.

The value of $\lambda = 6/5$ in Step 1 of Algorithm 1 is not the only value λ may assume for ensuring that the BBHT succeeds. It should be noted that λ should be greater than 1, since if $\lambda < 1$, then m in Step 10 of Algorithm 1 would eventually be almost zero, resulting in applying no Grover iterations. At the same time, λ should be smaller than $4/3$ for ensuring that the BBHT succeeds with a probability of $\sim$100% after $L_{BBHT}^{QD,\ \max} = O(\sqrt{N/S})$ CFEs in the QD [17]. This is true even in the worst-case scenario, where the maximum allowed value of $L = \lfloor m \rfloor = \left\lfloor \lambda^{u+\lceil \log_\lambda m_c \rceil} \right\rfloor$ is chosen during the $(u + \lceil \log_\lambda m_c \rceil)$th BBHT iteration associated with $u \geq 0$.

For $1 < \lambda < 4/3$, the BBHT will find a solution, if it does exist, and this is accomplished in the worst-case scenario at the cost of fewer CFEs in the QD than [17]

$$L_{BBHT}^{QD,\ \max} = \left(\frac{\lambda}{\lambda - 1} + \frac{\lambda}{4 - 3\lambda}\right) \cdot \frac{1}{2}\sqrt{\frac{N}{S}}. \quad (10)$$

Let us continue by using $\lambda = 6/5$ in Algorithm 1, for the reason that this value of λ minimizes the $L_{BBHT}^{QD,\ \max}$ in (10) and it corresponds to the minimum value of $L_{BBHT}^{QD,\ \max} = 4.5\sqrt{N/S}$.

Algorithm 1: BBHT Quantum Search Algorithm

1: Set $m \leftarrow 1$, $\lambda \leftarrow 6/5$ and $L_{BBHT}^{QD} \leftarrow 0$, $L_{BBHT}^{CD} \leftarrow 0$.
2: Choose L uniformly from the set $\{0, \ldots, \lfloor m \rfloor\}$.
3: Apply the $\mathcal{G}$ operator L times starting from the initial state $|x\rangle$ in (6), resulting in the final state $|x_f\rangle = \mathcal{G}^L|x\rangle$.
4: Observe $|x_f\rangle$ in the QD and obtain $|j\rangle$.
5: Compute $f(j)$ in the CD.
6: Update $L_{BBHT}^{CD} \leftarrow L_{BBHT}^{CD} + 1$ and $L_{BBHT}^{QD} \leftarrow L_{BBHT}^{QD} + L$.
7: **if** $f(j) = \delta$ or $L_{BBHT}^{QD} \geq L_{BBHT}^{QD,\ \max}$ **then**
8: Set $x_s \leftarrow j$, output x_s, L_{BBHT}^{CD}, L_{BBHT}^{QD} and exit.
9: **else**
10: Set $m \leftarrow \min\left\{\lambda m, \sqrt{N}\right\}$ and go to Step 2.
11: **end if**

C. Dürr-Høyer Algorithm

Without assuming any *a priori* knowledge about the output values of the CFEs, the DHA [18], [27] succeeds in finding the specific M^K-ary symbol $x_{\min}$ that minimizes the CF of (2) and (4) for DS-CDMA and SDMA systems, respectively, with $\sim$100% probability. The DHA is described in Algorithm 2 [27] with the differences that in Step 1 we have $L_{stop} = 22.5\sqrt{N}$ and i is randomly initialized from the set $\{0, \ldots, N-1\}$. It requires $22.5\sqrt{N}$ and $4.5\sqrt{N}$ Grover iterations in the worst-case and best-case scenarios, respectively [18]. The BBHT QSA is exploited by the DHA, albeit with the difference that the Oracle marks as solutions those particular states $|x\rangle$ that satisfy $f(x) < \delta$. When $x_s = x_{\min}$ naturally occurs in Step 2 of Algorithm 2, the DHA will not realize this in Step 4, therefore it would move to Step 7, ultimately leading to $4.5\sqrt{N}$ unnecessary CFEs in the following Step 2, since $x_{\min}$ has already been found.

D. Deterministically-initialized, Early-Stopping DHA

The proposed ES DHA is summarized in Algorithm 2. The differences with respect to the original DHA are two-fold. Firstly, in a DS-CDMA system the MF output x_{MF} is used as the initial input i in Step 1 of Algorithm 2 instead of i being randomly chosen from the set $\{0, \ldots, N-1\}$ with a

probability of $1/N$ as in the DHA. Similarly, in an SDMA system, the outputs of the ZF or the MMSE detectors might be used as initial inputs to the DHA. Secondly, a specific stopping condition is used in Step 4, which has to satisfy $L_{DHA} \geq L_{stop}$, where L_{DHA} is the total number of CFEs performed both in the CD according to (2) and (4) and in the QD according to the number of Oracle calls which evaluates the CF of (2) or (4) up to this point, while L_{stop} is the user-defined maximum number of iterations, instead of naturally stopping when $x_{\min}$ was found, whilst observing the upper limit of $L_{DHA}^{QD,\,\max} = 22.5\sqrt{N}$ Grover iterations.

The CF evaluations in Step 4 of Algorithm 2 have already been realized in the BBHT QSA in the CD, therefore they do not contribute to the complexity. However, when Step 2 is visited for the first time, the CF value of the initial guess is required. Since the number of CF evaluations performed by the BBHT QSA in the CD depends on the behaviour of the CFEs in the QD, we are only able to theoretically calculate the minimum number of CFEs performed in the CD, which corresponds to $L_{DHA}^{QD} = 4.5\sqrt{N}$ CFEs performed in the QD. The specific scenario, which gives the lowest number of CFEs in the CD assumes that the initial input i is equal to the solution $x_{\min}$. Hence, the BBHT QSA employed by the DHA will carry out at least $L_{DHA}^{QD} = 4.5\sqrt{N}$ Oracle operations, where $4.5\sqrt{N}$ is the minimum number of CFEs required in the QD for the DHA. According to Step 2 of Algorithm 1, the number of Grover iterations L is uniformly chosen from the set $\{0, \ldots, \lfloor m \rfloor\}$ at the beginning of each BBHT iteration, where m is updated according to $m \leftarrow \min\{\lambda m, \sqrt{N}\}$ and it is initialized to $m = 1$. Since $i = x_{\min}$, there are no solutions, hence naturally no solutions will be found. Therefore the sooner we reach $L_{BBHT}^{QD} = L_{BBHT}^{QD,\,\max} = 4.5\sqrt{N}$, the fewer CFEs have to be performed in the CD after each "guess" of the BBHT QSA in Steps 4 and 5 of Algorithm 1. The specific scenario that requires the minimum number of CFEs in the CD is the one, where L is chosen to be $\lfloor m \rfloor$ during each BBHT iteration. Therefore, the minimum number of CFEs in the CD $L_{DHA}^{CD,\,\min}$ for the DHA is

$$L_{DHA}^{CD,\,\min} = \min\left\{L_{DHA}^{CD}\right\} + 1 \quad (11)$$
$$s.t. \left[\sum_{j=0}^{L_{DHA}^{CD}-1} \min\left(\left\lfloor \lambda^j \right\rfloor, \sqrt{N}\right)\right] \geq 4.5\sqrt{N}.$$

The scenario that includes the total of the minimum number of CFEs in both the CD and the QD is the one, where $L_{DHA}^{CD,\,\min}$ iterations of the BBHT are performed and the total number of Grover iterations applied in these BBHT iterations is equal to $L_{BBHT}^{QD,\,\max} = 4.5\sqrt{N}$. One more CFE is added in (11) for evaluating the CF for the initial input of the DHA. For example, in a system where $N = 4$ and $\lambda = 6/5$, the minimum number of CFEs in the CD relying on (2) and (4) in the DHA is performed, when $x_{\min}$ is our initial guess and also when $L_{DHA}^{CD,\,\min} = 8$ according to (11). The minimum of the total number of CFEs is equal to 17 and this is achieved, when at the same time we had $L_{DHA}^{QD} = L_{BBHT}^{QD,\,\max} = 4.5\sqrt{N} = 9$ Oracle operations. This may occur, if L is chosen to be equal to 1 during the first 5 BBHT iterations, and then equal to 2 for the last two BBHT iterations, among other legitimate combinations. In general, the lower bound of the number of CFEs in the DHA is

$$\begin{aligned} L_{DHA}^{\min} &= L_{DHA}^{QD,\,\min} + L_{DHA}^{CD,\,\min} \\ &= L_{BBHT}^{QD,\,\max} + L_{DHA}^{CD,\,\min}, \end{aligned} \quad (12)$$

where $L_{BBHT}^{QD,\,\max} = 4.5\sqrt{N}$ and $L_{DHA}^{CD,\,\min}$ is given in (11).

The $L_{DHA}^{\min}$ CFEs based on (12) are required by the DHA for realizing that the solution has already been found [18], [27] and hence these CFEs may be considered redundant. A specific stopping condition of $L'_{stop} \geq L_{DHA}^{\min}$ may be defined based on the histogram acquired experimentally for approximating the Cumulative Density Function (CDF) of the number of CFEs required for achieving a certain probability of success in the DHA. For example, L'_{stop} may be set to the total number of CFEs required in both the CD and the QD for the DHA to succeed in finding $x_{\min}$ with a 60% probability. In this scenario, if we only allow $L_{stop} = L'_{stop} - L_{DHA}^{\min}$ CFEs instead of L'_{stop}, we should still expect a 60% probability of success, since the last $L_{DHA}^{\min}$ CFEs were only employed for allowing the DHA to realize that the solution has already been found. Based on the proposed techniques which will be analysed in the following, at least $L_{DHA}^{\min} = L_{DHA}^{QD,\,\min} + L_{DHA}^{CD,\,\min} = 4.5\sqrt{N} + L_{DHA}^{CD,\,\min}$ CFEs may be avoided, which substantially reduces the computational complexity in large-scale systems.

Algorithm 2: Deterministically-initialized, ES-aided DHA

1: Set the maximum allowed number of total CFEs L_{stop}. Furthermore, set $i \leftarrow x_I$ and $L_{DHA} \leftarrow 0$, $L_{DHA}^{CD} \leftarrow 0$, $L_{DHA}^{QD} \leftarrow 0$.
2: The BBHT QSA is employed with $\delta \leftarrow f(i)$, an Oracle that marks as solutions the states $|x\rangle$ that obey $f(x) < \delta$ and $L_{BBHT}^{\max} \leftarrow \min\{4.5\sqrt{N}, L_{stop} - L_{DHA}\}$, where $L_{BBHT}^{\max}$ refers to the total allowed number of CFEs in both the CD and the QD. Obtain x_s, L_{BBHT}^{CD} and L_{BBHT}^{QD} from the BBHT QSA.
3: $L_{DHA}^{CD} \leftarrow L_{DHA}^{CD} + L_{BBHT}^{CD}$, $L_{DHA}^{QD} \leftarrow L_{DHA}^{QD} + L_{BBHT}^{QD}$ and $L_{DHA} \leftarrow L_{DHA} + L_{DHA}^{CD} + L_{DHA}^{QD}$.
4: **if** $f(x_s) \geq f(i)$ or $L_{DHA} \geq L_{stop}$, **then**
5: Set $x_{\min} \leftarrow i$, output $x_{\min}$ and exit.
6: **else**
7: Set $i \leftarrow x_s$ and go to Step 2.
8: **end if**

IV. Design Methodology

In this section we present the design methodology of our proposed ES-aided DHA QMUD by employing it in both full-rank and in challenging rank-deficient DS-CDMA and SDMA systems, both having the same user load. In this context it is of paramount importance that conventional MUDs tend to exhibit a high residual BER in rank-deficient scenarios, even though these often occur in practice, unless the upper layers simply block or drop users requesting access in scenarios of $K > SF$ and $K > P$. Quantitatively, our full-rank DS-CDMA system supports $K = 15$ users in conjunction with Gold codes having $SF = 15$ chips, while the SDMA system supports $K = 15$ users with the aid of $P = 15$ receive antennas at the BS, resulting in a user load of $K/SF = K/P = 1$. By contrast,

TABLE I
NUMBER OF CFES OF THE SYSTEMS IN FIG. 2 AT THE E_b/N_0 VALUES PER RECEIVE ANTENNA CORRESPONDING TO A BER OF $\sim 10^{-5}$

	ML	DHA QMUD	DS-CDMA	SDMA
$K = 14$	16 384	$SF = P = 7$	10 dB	6.65 dB
		Minimum	604	604
		Average	967.26	914.72
		Maximum	2238	2181
$K = 15$	32 768	$SF = P = 15$	8 dB	4.96 dB
		Minimum	844	844
		Average	1016.1	1286.6
		Maximum	2352	2763

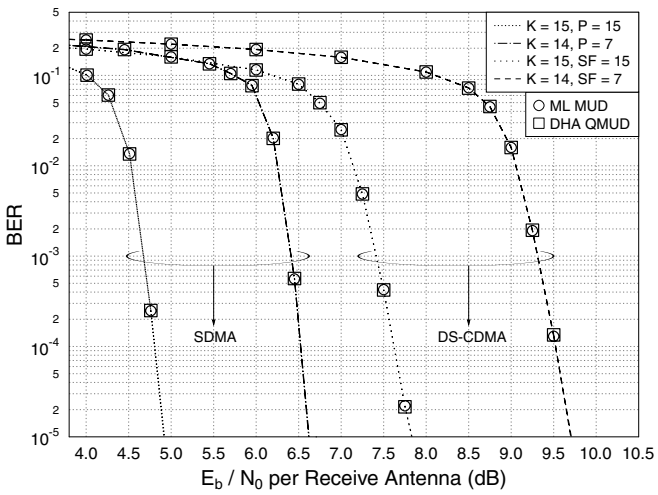

Fig. 2. BER performance with respect to the E_b/N_0 per receive antenna of DS-CDMA and SDMA systems supporting K users with SF chips in the spreading codes of the DS-CDMA systems and P receive antennas in the SDMA systems, employing BPSK modulation. The DHA is employed for performing optimal MUD. The bit-based interleavers' length is equal to 40 000 and 42 000 bits in the full-rank and the rank-deficient systems, respectively.

our rank-deficient DS-CDMA system supports $K = 14$ users employing m-sequences having $SF = 7$ chips, while $K = 14$ users are supported in the SDMA system using $P = 7$ receive antennas installed at the BS. Hence the normalized user load in the rank-deficient systems is $K/SF = K/P = 2$. In all four systems BPSK symbols associated with $M = 2$ were transmitted and Turbo Convolutional Codes (TCC) having a rate of R=1/2, 8 trellis states and 4 inner decoding iterations were used. The bit-based interleavers have a length of 40 000 bits and 42 000 bits in the full-rank and the rank-deficient systems, respectively. The specific E_b/N_0 values we will refer to are the E_b/N_0 values per receive antenna.

The BER performance of the $[K$=15$, SF$=15$]$, $[K$=15$, P$=15$]$, $[K$=14$, SF$=7$]$ and $[K$=14$, P$=7$]$ systems relying on the CD ML MUD and on the optimal DHA QMUD is presented in Fig. 2. The BER of the optimal DHA QMUD is equivalent to that of the ML MUD, but this is achieved at fewer CFEs, as seen in Table I. The DHA QMUD is deterministically-initialized, where the MF output was used as the initial input of the DHA in the DS-CDMA systems, while the ZF and MMSE detectors' outputs were used in the SDMA system for the rank-deficient and the full-rank scenarios, respectively. The full-rank $[K$=15, SF=15$]$ system performs by 1.87 dB better than the rank-deficient $[K$=14, SF=7$]$ system. This was indeed expected, since the Multi-User Interference (MUI) in the former system is lower owing to its lower normalized user-load of $K/SF = 1$, instead of $K/SF = 2$. A similar conclusion may be drawn for the full-rank and rank-deficient SDMA systems. As seen in Fig. 2, the full-rank SDMA system requires approximately 3.04 dB lower bit-energy per receive antenna than the full-rank DS-CDMA system supporting $K = 15$ users for achieving a BER of 10^{-5}. Please note again that the $[K$=14, SF=7$]$ and the $[K$=14, P=7$]$ scenarios are highly rank-deficient, hence conventional MMSE-style MUDs would result in a high residual BER.

In our proposed MUD application, the M^K-ary symbol x_{MF} at the MF output of the DS-CDMA systems will be the initial value of $i = x_{MF}$ in Step 1 of the ES-DHA, since the MF output has on average a lower Euclidean distance from the optimal M^K-ary symbol $x_{\min}$ than a randomly chosen one, hence requiring fewer iterations for both the DHA and therefore also for the BBHT QSA to reach $x_{\min}$. The dependence of the DHA's complexity on the initial value i chosen at its first step is illustrated in Fig. 3a, 3b, 3g, 3h, where both the simulation-based experimental histogram approximating the Probability Density Function (PDF) and the corresponding Cumulative Density Function (CDF) of the DHA's total CFEs are presented for the systems investigated. Moreover, the PDF and CDF curves of the CFEs performed in the QD and CD are also given for the rank-deficient systems in Fig. 3c, 3d, 3e, 3f. The randomly-initialized DHA QMUD has a similar PDF and CDF for the DS-CDMA and SDMA systems for the same search space size, verifying that the randomly-initialized DHA's complexity depends solely on the number of users and on the number of bits/symbol used, but not on the operating E_b/N_0 value or on the multiple access scheme used, in terms of the SF value, or the number of receive antennas P employed. The CDF curves of the randomly-initialized DHA provide the upper limit for the complexity of the QMUD, since in the worst-case scenario the conventional detectors will output random symbols. The complexity reduction achieved by the deterministically-initialized DHA with respect to the complexity of the randomly-initialized DHA varies as a function of the SF, E_b/N_0, the number of receive antennas P, as well as the channel, but it is almost always non-negligible, as illustrated in Fig. 3, except when the conditions are so severe that essentially turn the conventional detector into a random symbol generator. Moreover, the PDF of the total number of CFEs performed in both the CD and QD in the DHA is the convolution of the number of CFEs performed in the CD and the number of Grover iterations, as it may be seen in Fig. 3b, 3d and 3f for the rank-deficient SDMA system.

Again, the last $L_{DHA}^{QD,\,\min}$=$4.5\sqrt{M^K}$ Grover operations in the DHA are purely required by the DHA in order to realize that $x_{\min}$ has already been found, rather than to actually find it. Hence, if we have $i = x_{\min}$, then only $L_{DHA}^{\min}$ CFEs of (12) will be performed, representing the lower limit in the DHA and explaining the reason that the probability of finding

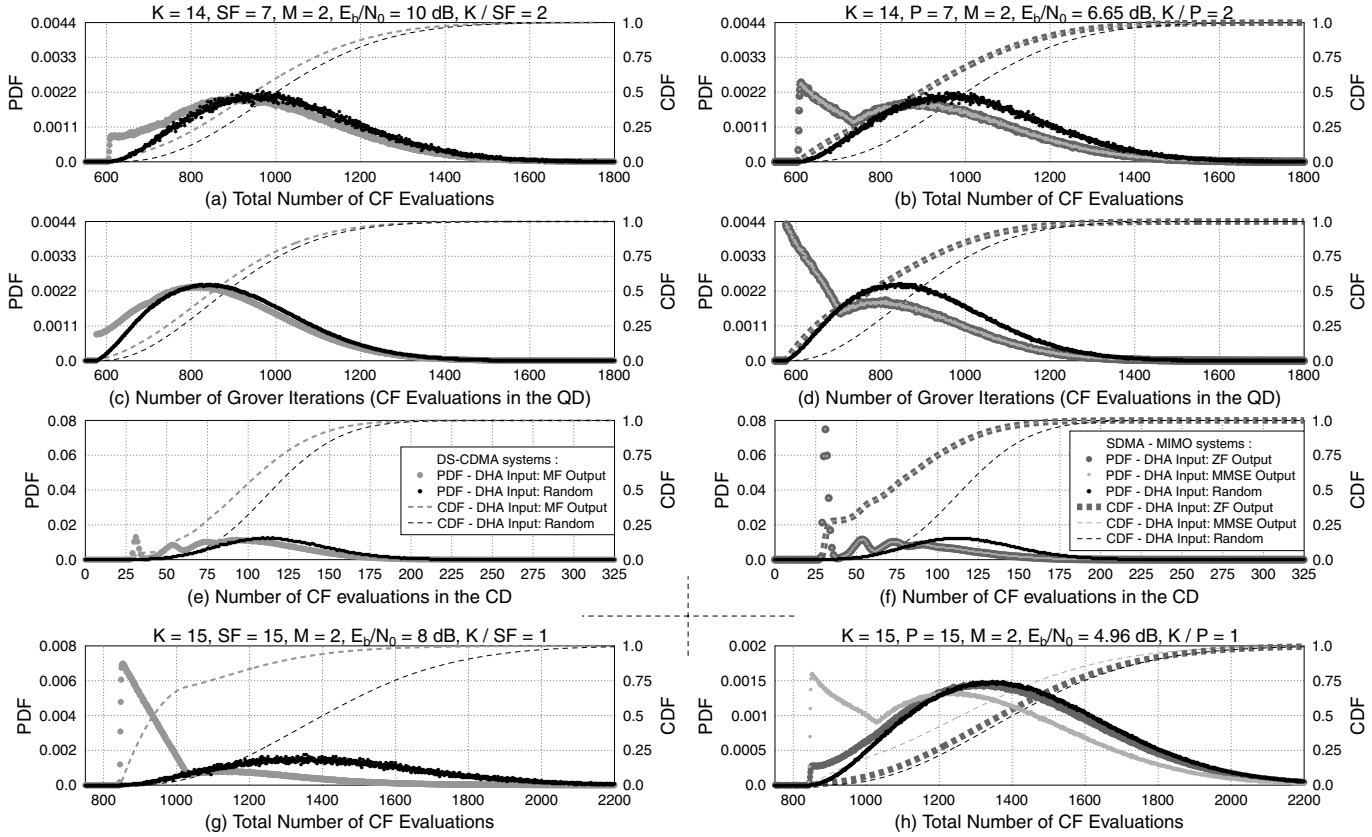

Fig. 3. Simulated PDF and CDF of the total number of CFEs in the DHA employed in the (a) $[K{=}14, SF{=}7]$ DS-CDMA system, (b) $[K{=}14, P{=}7]$ SDMA system. The corresponding PDF and CDF curves of the number of CFEs performed in the quantum domain are presented in (c) and (d) for the $[K{=}14, SF{=}7]$ DS-CDMA system and the $[K{=}14, P{=}7]$ SDMA system, respectively, while the PDF and CDF curves of the number of CFEs performed in the classic domain are illustrated in (e) and (f) for the two systems, respectively. The PDF and CDF curves of the total number of CFEs in the DHA employed in the $[K{=}15, SF{=}15]$ DS-CDMA system and the $[K{=}15, P{=}15]$ SDMA system are depicted in (g) and (h), respectively. The chosen E_b/N_0 per receive antenna values correspond to a BER of $\sim 10^{-5}$.

$x_{\min}$ with less than $L_{DHA}^{\min} = 604$ CFEs in the simulated PDF curves seen in Fig. 3a, 3b is equal to zero. The same applies for the full-rank systems of Fig. 3g and 3h, where $L_{DHA}^{\min} = 844$ CFEs are required according to (12). Since $x_{MF} = x_{\min}$ is a common occurrence in full-rank DS-CDMA systems [1], such as the fully-loaded system of Fig. 3g associated with $K/SF = 1$, we observe a peak in its PDF at $L_{DHA} = L_{DHA}^{\min}$ CFEs for $i = x_{MF}$. On the other hand, for the rank-deficient systems, such as the ones characterized in Fig. 3a and Fig. 3b, where we have $K/SF > 1$ and $K/P > 1$, respectively, we may observe that the MF, ZF and MMSE outputs are closer to a random guess of the transmitted M^K-ary symbol.

The CDF curves seen in Fig. 3 are also shifted towards the lower CFE limit of the DHA, when we have deterministically-initialized i, indicating the complexity reduction achieved. Observe that in the full-rank scenario of Fig. 3g, the shift of the MF-initialized system's CDF is more substantial than that of the MF-initialized rank-deficient DS-CDMA scenario. The specific E_b/N_0 per receive antenna value, where each system was investigated in Fig. 3 corresponds to a BER of $\sim 10^{-5}$, since practical systems are desired to operate in that region. It is expected that the PDF and CDF curves will be further shifted towards fewer CFEs, when the E_b/N_0 is increased, since the event of $i = x_{MF} = x_{\min}$ in the DS-CDMA and $i = x_{MMSE} = x_{\min}$ in the SDMA systems will become more frequent even in rank-deficient systems. The CDF curves recorded for the $[K{=}15,\ SF{=}15]$ and $[K{=}15,\ P{=}15]$ systems in Fig. 4 verify our expectations. According to the CDF curves seen in Fig. 4, given at the same bit power per receive antenna of 10 dB, namely when an SDMA and a DS-CDMA system supporting the same number of users and employing the same modulation scheme operate at the same power level, the deterministically-initialized DHA used in the DS-CDMA system would require fewer CFEs to find $x_{\min}$. For example, for the sake of achieving 75% detection success probability, when the DS-CDMA and the SDMA systems support $K = 15$ users associated with $SF = 15$ chips and $P = 15$ receive antennas, respectively, at an E_b/N_0 per receive antenna value of 10 dB, the DHA requires 1047 CFEs in the DS-CDMA systems and 1347 CFEs in the SDMA system according to Fig. 4a and 4b, respectively.

The CDF shift seen in Fig. 4a is small, when operating in the desired power region of the $[K{=}14,\ SF{=}7]$ system, where the BER is sufficiently low. Similarly, the CDF shift seen in Fig. 4b is also low – approximately 10 CFEs per 0.6 dB power increase. Based on the gradually-shifting nature of the CDFs with respect to power, we can benefit from an early stopping of the DHA. For example, if we stop the

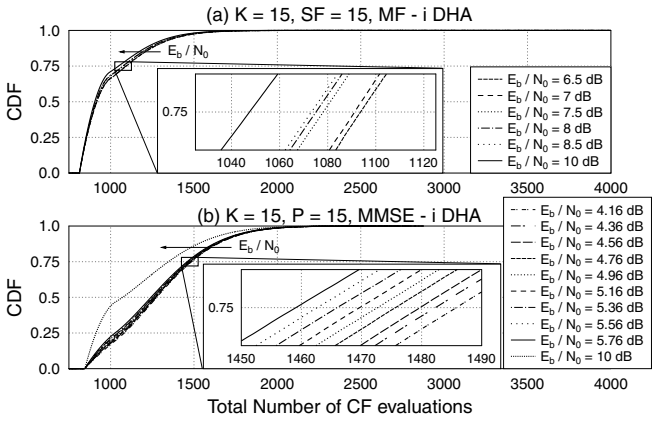

Fig. 4. Simulated CDF curves of the number of CFEs in the DHA employed in the (a) $[K{=}15,\ SF{=}15]$ and (b) $[K{=}15,\ P{=}15]$ systems using BPSK modulation for various values of E_b/N_0 per receive antenna.

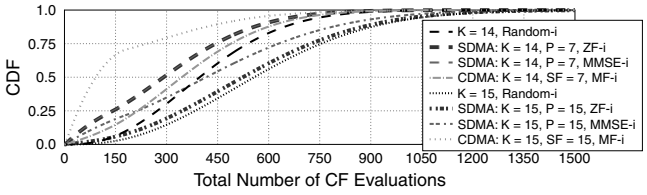

Fig. 5. Simulated CDF curves of the number of CFEs in the DHA employed in the $[K{=}14,\ SF{=}7]$, $[K{=}14,\ P{=}7]$, $[K{=}15,\ SF{=}15]$ and $[K{=}15,\ P{=}15]$ systems employing BPSK modulation for E_b/N_0 per receive antenna equal to 10 dB, 6.65 dB, 8 dB and 4.96 dB, respectively, where $L_{DHA}^{\min} = 604$ CFEs and 844 CFEs have been subtracted from the systems supporting $K = 14$ and $K = 15$ users, respectively.

MMSE-initialized DHA of the $[K{=}15,\ P{=}15]$ system after $L_{stop} = 1473$ CFEs, we will expect the DHA to find $x_{\min}$ in 75% of the instances for $E_b/N_0 = 4.96$ dB according to the CDF of Fig. 4b. Furthermore, we may eliminate the redundant $L_{DHA}^{\min}$ number of CFEs without any degradation of the BER performance. The maximum number of CFEs required for achieving a specific probability of success may be visually presented as in Fig. 5, where the CDF point corresponding to $L_{DHA}^{\min}$ CFEs in Fig. 3 is mapped to 0 CFEs in Fig. 5 and the rest of the points are mapped accordingly. Hence, if say 75% of detection success is desired at an E_b/N_0 per receive antenna of 4.96 dB in the system of Fig. 4b, this may be achieved by employing the ES-DHA at the expense of $L_{DHA}^{75\%,10\text{ dB}} - L_{DHA}^{\min} = 1473 - 844 = 629$ CFEs, as illustrated in Fig. 5. If the different CDF curves associated with each operating E_b/N_0 value are available, the probability of achieving the target BER may be estimated. In our simulations we will only rely on the CDFs of the systems evaluated at the power levels corresponding to a BER of $\sim 10^{-5}$, which are presented in Fig. 3. Again, the SDMA systems operate at a lower power level than the DS-CDMA systems supporting the same user-load ratios.

The design procedure of the proposed ES-DHA QMUD may commence by generating the CDF curves of the randomly-initialized DHA, which do not depend on the channel, on the number of receive antennas, the value of SF, or the E_b/N_0 value, but only on the number of users K and on the specific choice of the M-ary modulation employed, which determine the size M^K of the search problem. Therefore, the CDF curve obtained by employing the randomly-initialized DHA for finding the index of the minimum entry in a database having M^K randomly generated entries is the same as if the CDF curve of the randomly-initialized DHA was generated based on the channel probabilities of the communication system. Moreover, the complexity of determining the CDFs of the randomly-initialized DHA when invoked for a database having randomly generated entries is much lower, since there is no need for employing K encoding and decoding procedures, as well as K bit stream generations, symbol mapping and transmissions over fading channels. The CDF of the randomly-initialized DHA provides an upper limit for the complexity of the QMUD.

The design methodology is straightforward, since the ES-DHA QMUD may be flexibly set to the required number of CFEs. When approaching the optimal ML performance is the ultimate target, the design may commence by deciding upon the power levels the system's power control will have to operate at. Subsequently, the CDF curve of the deterministically-initialized DHA should be determined by off-line simulations at a power close to the chosen one. By observing the CDF curve generated after subtracting the number of CFEs $L_{DHA}^{\min}$ required by the DHA for realizing that the solution has already been found in (12), the maximum number of CFEs L_{stop} corresponding to the desired point of the CDF may be extracted. Employing the ES-DHA QMUD and stopping it after the predetermined number of L_{stop} CFEs statistically-speaking guarantees the required performance at a low and fixed complexity even in highly rank-deficient systems, when powerful turbo codes are used for correcting the majority of the remaining detection errors.

The design methodology would depend on the maximum tolerable complexity quantified in terms of the maximum number of CFEs. By examining the pre-stored CDF of the randomly-initialized DHA, the expected probability of success may be found. If the probability of success is unsatisfactory, we may employ deterministically-initialized DHA. Consulting a pre-stored CDF curve for a specific operational E_b/N_0 value will lead us to conclusions regarding the probability of success, which will be higher than that of the randomly-initialized DHA. If the updated probability of success remains unsatisfactory, we may increase the power level. If the probability of success exceeds the design specifications, we may either choose to operate at a lower power, or reduce the complexity invested, in order to "just" satisfy our desired probability of success.

V. Performance Versus Complexity

Based on the previous observations and the CDF curves of Fig. 5, in Table II we have gathered the maximum number of CFEs required by each investigated system for achieving a certain probability of success in finding $x_{\min}$ using the proposed deterministically-initialized ES-DHA. In Fig. 6 and Fig. 7 we considered the BER performance of both the rank-deficient and full-rank systems, respectively, where the ES-DHA was stopped after L_{stop} iterations appropriately chosen from Table II. More precisely, according to Table II, for the $[K{=}15,\ SF{=}15]$ system we may infer that 99% of the

TABLE II
NUMBER OF CFES OF THE SYSTEMS IN FIG. 6 AND FIG. 7 REQUIRED FOR ACHIEVING A SPECIFIC SUCCESS PROBABILITY IN THE DHA.

CDF %	$K=14$ $SF=7$ @ 10 dB	$K=15$ $SF=15$ @ 8 dB	$K=14$ $P=7$ @ 6.65 dB	$K=15$ $P=15$ @ 4.96 dB
99%	881	827	854	1200
90%	628	461	590	832
80%	527	310	484	685
70%	456	175	410	175
60%	397	122	348	496
50%	345	93	292	418

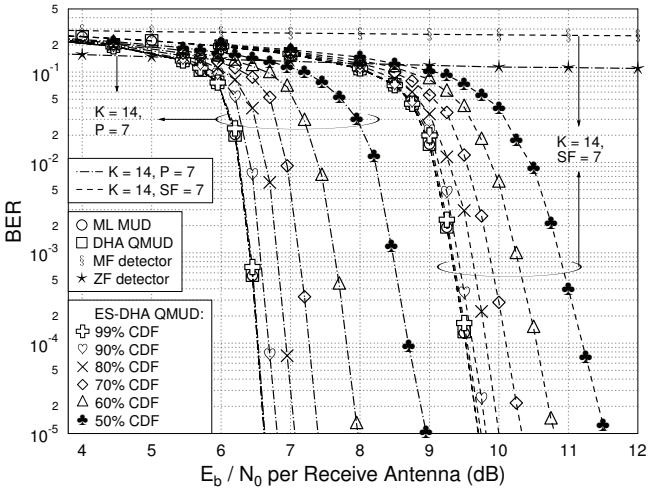

Fig. 6. BER performance with respect to the E_b/N_0 per receive antenna of the rank-deficient DS-CDMA system supporting $K = 14$ users with $SF = 7$ chips and SDMA system supporting $K = 14$ users with $P = 7$ receive antennas, with the stopping points of the ES-aided DHA QMUD having been chosen based on the fractions of the corresponding CDFs of Fig. 3 and they are given in Table II. The $[K{=}14,\ P{=}7]$ system employs ZF-initialized ES-DHA QMUD while the MF-initialized ES-DHA QMUD is applied in the rank-deficient DS-CDMA system. Both systems employ TCC with rate $R{=}1/2$, relying on 8 trellis states, 4 inner decoding iterations and the bit-based interleavers have a length of 42 000 bits.

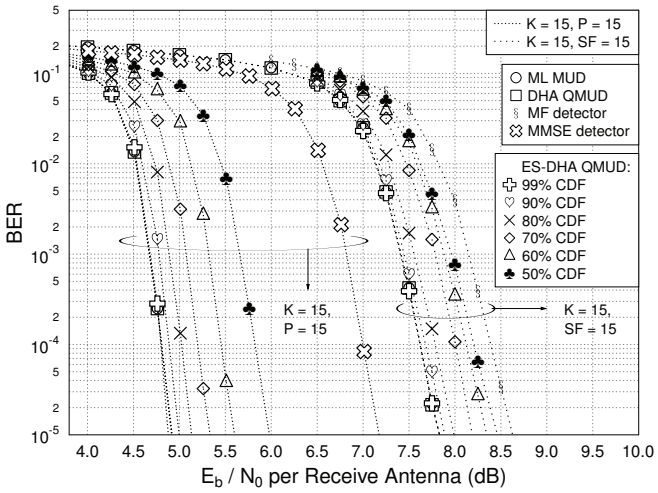

Fig. 7. BER performance with respect to the E_b/N_0 per receive antenna of the full-rank DS-CDMA system supporting $K = 15$ users with $SF = 15$ chips and SDMA system supporting $K = 15$ users with $P = 15$ receive antennas, with the stopping points of the ES-aided DHA QMUD having been chosen based on the fractions of the corresponding CDFs of Fig. 3 and they are given in Table II. The $[K{=}15,\ P{=}15]$ system employs MMSE-initialized ES-DHA QMUD while the MF-initialized ES-DHA QMUD is applied in the full-rank DS-CDMA system. Both systems employ TCC with rate $R{=}1/2$, relying on 8 trellis states, 4 inner decoding iterations and the bit-based interleavers have a length of 40 000 bits.

instances require less than $L_{DHA}^{99\%,8\text{ dB}} = 827$ CFEs. Hence we expect the performance associated with $L_{stop} = 827$ CFEs to be the same as that of the optimal DHA QMUD, where we have $L_{stop} = 22.5\sqrt{M^K} = 4072$ Grover iterations and the maximum number of CFEs required for the detection of an M^K-ary symbol in our simulations was 2352 CFEs. Therefore, by using the proposed ES-aided DHA we match the performance of the ML MUD, as seen in Fig. 7, while eliminating the randomly appearing high peaks in its search-complexity. In fact, in the $[K{=}15,\ SF{=}15]$ system we achieve the optimal ML performance at a complexity below the lower limit of the optimal DHA. The optimal ML performance is also achieved in the rank-deficient systems of Fig. 6, provided that their specific numbers of CFEs associated with 99% detection success probability are used from Table II.

Following the same methodology, in Fig. 6 and 7 we have also evaluated the BER performance of both the fully-loaded and of the rank-deficient DS-CDMA and SDMA systems, respectively, while imposing specific complexity limits on the DHA. The ES-DHA QMUD was MMSE-initialized in the full-rank SDMA system of Fig. 7, since this was found to provide a better initial estimate according to Fig. 3h, while the ES-DHA QMUD of the rank-deficient SDMA system of Fig. 6 was ZF-initialized. Both DS-CDMA systems employ MF-initialized ES-DHA QMUDs. As expected, the achievable performance degrades, when the DHA is stopped earlier than it naturally would, because in some of the cases only a sub-optimal solution will have been found. Comparing Fig. 6 to Fig. 7, the degradation experienced is higher for the rank-deficient systems. Furthermore, the DS-CDMA systems experience a lower degradation, when operating at the same success probability point of their respective CDF curves in both full-rank and rank-deficient systems. When operating at lower CDF points, the BER performance approaches that of the initial detector, since the 0% point of the CDF corresponds to having an output constituted by the initial "guess". It may be verified by the full-rank systems characterized in Fig. 7 that indeed this is the case, while the performance of the rank-deficient systems in Fig. 6 operating at the 50% points of their respective CDF curves is still adequate, when compared to the conventional detectors' performance, both of which have a high residual BER. If an even lower CDF point was chosen in a rank-deficient system, a high residual BER would also appear.

The E_b/N_0 loss versus the reduction in complexity is illustrated in Fig. 8. As the number of CFEs increases, the performance loss diminishes. The SDMA systems may require more CFEs for approaching their optimal performance, especially when they operate at a low power, as observed in Fig. 8 for our full-rank SDMA scenario, because at low SNRs the conventional detectors fail to provide an accurate initial estimate of the M^K-ary symbol. Hence, depending both on

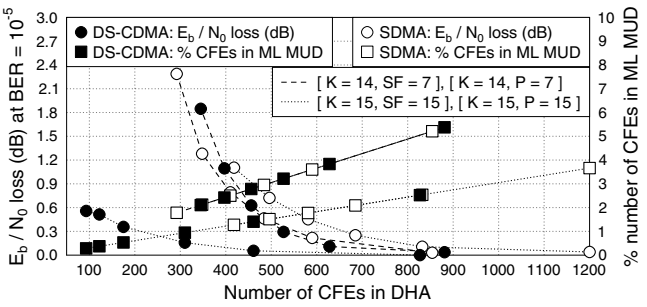

Fig. 8. Illustration of the power loss and the simultaneous reduction in complexity in the full-rank and rank-deficient DS-CDMA and SDMA systems with respect to the maximum allowed CFEs in the ES-aided DHA QMUD when compared to that of the ML MUD, and when TCC associated with R=1/2, relying on 8 trellis states and 4 inner iterations is used. The bit-based interleavers have a length of 40 000 and 42 000 bits each for the systems supporting $K = 15$ and $K = 14$ users, respectively.

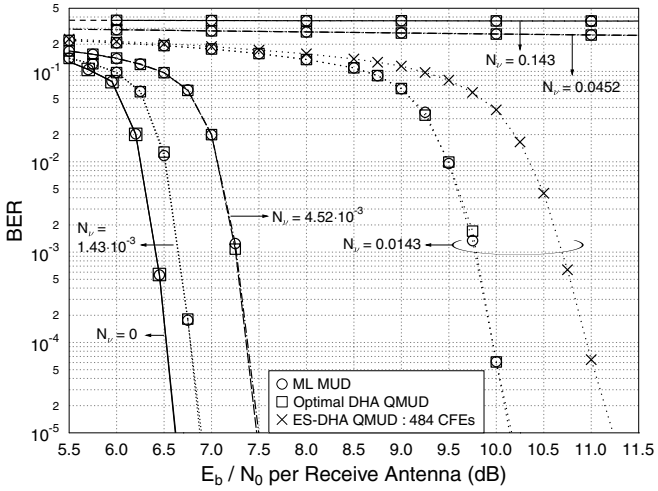

Fig. 9. BER performance with respect to the E_b/N_0 per receive antenna of the rank-deficient SDMA system supporting $K = 14$ users associated with $P = 7$ receive antennas when imperfect channel estimation is available. The CSI estimation noise variance N_ν describes the channel estimation error with $N_\nu = 0$ corresponding to perfect CSI estimation. The ML MUD, DHA QMUD and ES-aided DHA QMUD are employed and TCC associated with R=1/2, relying on 8 trellis states and 4 inner iterations is used. The bit-based interleavers have a length of 42 000 bits each.

the specific applications considered and on the computational power available, an adaptive strategy of choosing L_{stop} may be conceived.

In Fig. 9 we also considered the rank-deficient SDMA system in the realistic scenario where perfect estimation of the CSI is unavailable. We corrupted the perfect CSI with AWGN as in

$$\tilde{h}_{k,p} = h_{k,p} + \nu, \tag{13}$$

where h is the complex-valued channel coefficient depicted in Fig. 1b, with $k \in \{, \ldots, K-1\}$, $p \in \{0, \ldots, P-1\}$, and ν is the zero-mean and N_ν-variance AWGN noise. The imperfect channel estimation's error is described by the associated noise variance, where $N_\nu = 0$ denotes perfect channel estimation. The average channel power is the inverse of the number of the receive antennas $\gamma_c = 1/P$. According to Fig. 9, the DHA QMUD continues to have optimal ML performance even with imperfect channel estimation. On the other hand, when the ES-DHA QMUD is stopped after 484 CFEs, which corresponds to the 80% CDF point of the same system at an E_b/N_0 per receive antenna value of 6.65 dB and using perfect channel estimation based on Table II, the performance is approximately 1.1 dB away from that of the ML MUD. By contrast, in the $[K$=14, P=7] system relying on perfect channel estimation shown in Fig. 8 the degradation was just 0.45 dB. This was expected, since imperfect channel estimation results in a worse initial guess from the ZF detector, therefore requiring more CFEs in the DHA to find the optimum M^K-ary symbol. In other words, the CDF is shifted to the right and the simulated curve at 484 CFEs corresponds to a success probability below 80%. We may conclude that our proposed ES-DHA QMUD depends on the accuracy of the channel estimation.

VI. Conclusions

An ES-aided DHA-based QMUD was proposed for challenging rank-deficient DS-CDMA and SDMA scenarios operating at a normalized user-load of $L_u = 2$ and at a fixed complexity, which is lower than that of the variable complexity of the DHA-based QMUD of [27]. The fixed complexity of the ES-DHA QMUD may be flexibly tuned for diverse applications. The proposed ES-DHA may also be used in the SISO QMUD of [27] for reducing its total complexity, as well as in any other applications for which the CDF of the number of CFEs is available.

References

[1] L. Hanzo, L.-L. Yang, E.-L. Kuan, and K. Yen, *Single and Multi-Carrier DS-CDMA: Multi-User Detection, Space-Time Spreading, Synchronisation, Networking, and Standards*. John Wiley & Sons, 2003.

[2] L. Hanzo, O. Alamri, M. El-Hajjar and N. Wu, *Near-Capacity Multi-Functional MIMO Systems: Sphere-Packing, Iterative Detection and Cooperation*. John Wiley & Sons, IEEE Press, May 2009.

[3] L. Hanzo, Y. Akhtman, M. Jiang, and L. Wang, *MIMO-OFDM for LTE, WIFI and WIMAX: Coherent versus Non-Coherent and Cooperative Turbo-Transceivers* . John Wiley & Sons, 2010.

[4] Y. Li, J. Winters, and N. Sollenberger, "MIMO-OFDM for wireless communications: signal detection with enhanced channel estimation," *IEEE Trans. Commun.*, vol. 50, no. 9, pp. 1471–1477, 2002.

[5] X. Xu, R. Zhang, S. Ghafoor, and L. Hanzo, "Imperfect digital-fiber-optic-link-based cooperative distributed antennas with fractional frequency reuse in multicell multiuser networks," *IEEE Trans. Veh. Technol.*, vol. 60, no. 9, pp. 4439–4449, 2011.

[6] Z. Shen, J. Andrews, and B. Evans, "Adaptive resource allocation in multiuser OFDM systems with proportional rate constraints," *IEEE Trans. Wireless Commun.*, vol. 4, no. 6, pp. 2726–2737, 2005.

[7] J. Huang, V. Subramanian, R. Agrawal, and R. Berry, "Joint scheduling and resource allocation in uplink OFDM systems for broadband wireless access networks," *IEEE J. Sel. Areas Commun.*, vol. 27, no. 2, pp. 226–234, 2009.

[8] M. Pischella and J. C. Belfiore, "Distributed resource allocation for rate-constrained users in multi-cell OFDMA networks," *IEEE Commun. Lett.*, vol. 12, no. 4, pp. 250–252, 2008.

[9] Y. Yuan, Z. He, and M. Chen, "Virtual MIMO-based cross-layer design for wireless sensor networks," *IEEE Trans. Veh. Technol.*, vol. 55, no. 3, pp. 856–864, 2006.

[10] H. Wang, Y. Yang, M. Ma, J. He, and X. Wang, "Network lifetime maximization with cross-layer design in wireless sensor networks," *IEEE Trans. Wireless Commun.*, vol. 7, no. 10, pp. 3759–3768, 2008.

[11] H. Wang, N. Agoulmine, M. Ma, and Y. Jin, "Network lifetime optimization in wireless sensor networks," *IEEE J. Sel. Areas Commun.*, vol. 28, no. 7, pp. 1127–1137, 2010.

[12] G. Shirazi and L. Lampe, "Lifetime maximization in UWB sensor networks for event detection," *IEEE Trans. Signal Process.*, vol. 59, no. 9, pp. 4411–4423, 2011.

[13] M. A. Nielsen and I. L. Chuang, *Quantum Computation and Quantum Information*. Cambridge University Press, 2000.
[14] S. Imre and F. Balázs, *Quantum Computing and Communications: An Engineering Approach*. John Wiley & Sons, 2005.
[15] S. Imre and L. Gyongyosi, *Advanced Quantum Communications: An Engineering Approach*. John Wiley & Sons, 2013.
[16] L. K. Grover, "A fast quantum mechanical algorithm for database search," in *Proc. 1996 ACM Symposium on the Theory of Computing*, pp. 212–219.
[17] M. Boyer, G. Brassard, P. Høyer, and A. Tapp, "Tight bounds on quantum searching," *Fortschritte der Physik*, vol. 46, pp. 493–506, 1998.
[18] C. Durr and P. Høyer, "A quantum algorithm for finding the minimum," eprint arXiv:quant-ph/9607014, July 1996.
[19] A. Malossini, E. Blanzieri, and T. Calarco, "Quantum genetic optimization," *IEEE Trans. Evolutionary Computation*, vol. 12, pp. 231–241, Apr. 2008.
[20] S. Moshavi, "Multi-user detection for DS-CDMA communications," *IEEE Communn. Mag.*, pp. 124–136, Oct. 1996.
[21] S. Chen, A. Livingstone, and L. Hanzo, "Minimum bit-error rate design for space-time equalization-based multiuser detection," *IEEE Trans. Commun.*, vol. 54, pp. 824–832, May 2006.
[22] C. Xu, R. Maunder, L.-L. Yang, and L. Hanzo, "Near-optimum multiuser detectors using soft-output ant-colony-optimization for the DS-CDMA uplink," *IEEE Signal Process. Lett.*, vol. 16, pp. 137–140, Feb. 2009.
[23] R. Zhang and L. Hanzo, "Iterative multiuser detection and channel decoding for DS-CDMA using harmony search," *IEEE Signal Process. Lett.*, vol. 16, no. 10, pp. 917–920, 2009.
[24] C. Ergun and K. Hacioglu, "Multiuser detection using a genetic algorithm in CDMA communications systems," *IEEE Trans. Commun.*, vol. 48, pp. 1374–1383, Aug. 2000.
[25] K. Yen and L. Hanzo, "Antenna-diversity-assisted genetic-algorithm-based multiuser detection schemes for synchronous CDMA systems," *IEEE Trans. Commun.*, vol. 51, pp. 366–370, Mar. 2003.
[26] S. Imre and F. Balázs, "Non-coherent multi-user detection based on quantum search," in *Proc. 2002 IEEE International Conference on Communications*, vol. 1, pp. 283–287.
[27] P. Botsinis, S. X. Ng, and L. Hanzo, "Quantum search algorithms, quantum wireless, and a low-complexity maximum likelihood iterative quantum multi-user detector design," *IEEE Access*, vol. 1, pp. 94–122, 2013. Available: http://ieeexplore.ieee.org/xpl/articleDetails.jsp?arnumber=6515077.

Panagiotis Botsinis (S'12) received his 5-year diploma, equivalent to the M.Eng. degree, from the School of Electrical and Computer Engineering of the National Technical University of Athens (NTUA), Greece, in 2010 and the M.Sc. degree in Wireless Communications with distinction from the University of Southampton, UK, in 2011. He is currently working towards the Ph.D. degree in the Communications, Signal Processing and Control (CSPC) group at the School of Electronics and Computer Science of the University of Southampton, UK. Since October 2010, he has been a member of the Technical Chamber of Greece. His research interests include quantum-assisted communications, iterative detection, MIMO, coded modulation, channel coding, cooperative communications, as well as combinatorial optimization.

Dr Soon Xin Ng (S'99-M'03-SM'08) received the B.Eng. degree (First class) in electronics engineering and the Ph.D. degree in wireless communications from the University of Southampton, Southampton, U.K., in 1999 and 2002, respectively. From 2003 to 2006, he was a postdoctoral research fellow working on collaborative European research projects known as SCOUT, NEWCOM and PHOENIX. Since August 2006, he has been a member of academic staff in the School of Electronics and Computer Science, University of Southampton. He is involved in the OPTIMIX and CONCERTO European projects as well as the IU-ATC and UC4G projects. He is currently a senior lecturer at the University of Southampton.

His research interests include adaptive coded modulation, coded modulation, channel coding, space-time coding, joint source and channel coding, iterative detection, OFDM, MIMO, cooperative communications, distributed coding, quantum error correction codes and joint wireless-and-optical-fiber communications. He has published over 150 papers and co-authored two John Wiley/IEEE Press books in this field. He is a Senior Member of the IEEE, a Chartered Engineer and a Fellow of the Higher Education Academy in the UK.

Lajos Hanzo (http://www-mobile.ecs.soton.ac.uk) FREng, FIEEE, FIET, Fellow of EURASIP, DSc received his degree in electronics in 1976 and his doctorate in 1983. In 2009 he was awarded the honorary doctorate "Doctor Honoris Causa" by the Technical University of Budapest. During his 35-year career in telecommunications he has held various research and academic posts in Hungary, Germany and the UK. Since 1986 he has been with the School of Electronics and Computer Science, University of Southampton, UK, where he holds the chair in telecommunications. He has successfully supervised 80 Ph.D. students, co-authored 20 John Wiley/IEEE Press books on mobile radio communications totalling in excess of 10 000 pages, published 1300+ research entries at IEEE Xplore, acted both as TPC and General Chair of IEEE conferences, presented keynote lectures and has been awarded a number of distinctions. Currently he is directing a 100-strong academic research team, working on a range of research projects in the field of wireless multimedia communications sponsored by industry, the Engineering and Physical Sciences Research Council (EPSRC) UK, the European IST Programme and the Mobile Virtual Centre of Excellence (VCE), UK. He is an enthusiastic supporter of industrial and academic liaison and he offers a range of industrial courses. He is also a Governor of the IEEE VTS. During 2008 – 2012 he was the Editor-in-Chief of the IEEE Press and a Chaired Professor also at Tsinghua University, Beijing. His research is funded by the European Research Council's Senior Research Fellow Grant. For further information on research in progress and associated publications please refer to http://www-mobile.ecs.soton.ac.uk. He has 16000+ citations.